nature research

https://doi.org/10.1038/s41577-020-00471-1

Supplementary information

Measuring immunity to SARS-CoV-2 infection: comparing assays and animal models

In the format provided by the authors and unedited

Khoury et al, *Measuring immunity to SARS-CoV-2 infection: comparing assays and animal models.*

Supplementary Information

Supplementary Box 1:

Translation from animal models to protective efficacy in humans

The concentration of antibody required to protect an individual from infection will increase with the inoculum size. In animal studies high inoculum sizes (10^4 to 10^6 infectious units) are commonly used. Although the average viral dose a human encounters in community transmission is unknown, it is likely much lower than the dose used in animal studies. Therefore, if one has achieved 80% protective efficacy with a certain antibody concentration in an animal study, then a lower concentration of the same antibody would theoretically be required to achieve the same efficacy in human community transmission (Supplementary Box 1 Figure 1). The fold-reduction in antibody concentration that will achieve the same protective efficacy in humans depends on the Hill coefficient of the concentration-inhibition curve from a pseudovirus assay, with a bigger scaling factor being required for less steep relationships*.

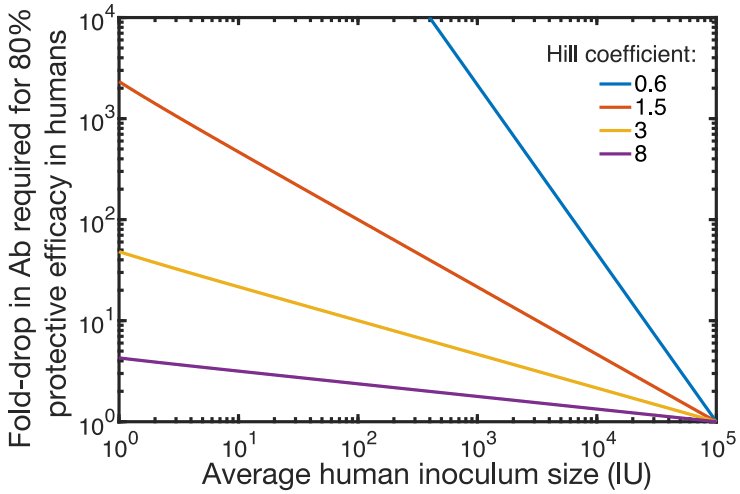

Supplementary Box 1, Figure 1: The fold reduction in the concentration of an antibody that would be required to achieve the same protective efficacy (of 80%) in human transmission compared with a high dose (10^5 IU) animal challenge model. This fold reduction depends on the average human inoculum size (which is not known but likely less than the dose used in animal studies, assumed here to be 10^5 IU), and the Hill coefficient of the concentration-inhibition curve from an *in vitro* pseudoviral inhibition assay.

* More generally the fold reduction in antibody concentration required for a protection level (ie: vaccine efficacy) of *P* is given by $R = \left(\frac{P^{1/I_A}}{P^{1/I_H}}\frac{1-P^{1/I_H}}{1-P^{1/I_A}}\right)^{1/H}$, where I_A and I_H are the average inoculum used in the animal study and the human inoculum size respectively, and H is the Hill coefficient.

Supplementary Box 2:

The effects of high inoculum on viral-immune dynamics

A high initial inoculum may act to shorten the time to peak viral load and affect the relative timing of viral and immune dynamics. In human infection it is thought a 'cytokine storm' evolving later in infection is central to much of the pathogenesis of severe disease. In most cases, this appears to arise as viral levels in the upper airways are declining (Suppl Box 2 Figure panel A). Higher inocula and more rapid declines in viral levels in some animal models may act to separate the timing of the peak of virus and immune response in these models (Figure panel B).

Recall responses after vaccination should act to accelerate the development of the host response, leading to earlier control of viral replication (Panel C). However, higher inocula may reduce the time window in which recall responses can act to effectively slow viral growth (Figure panel D).

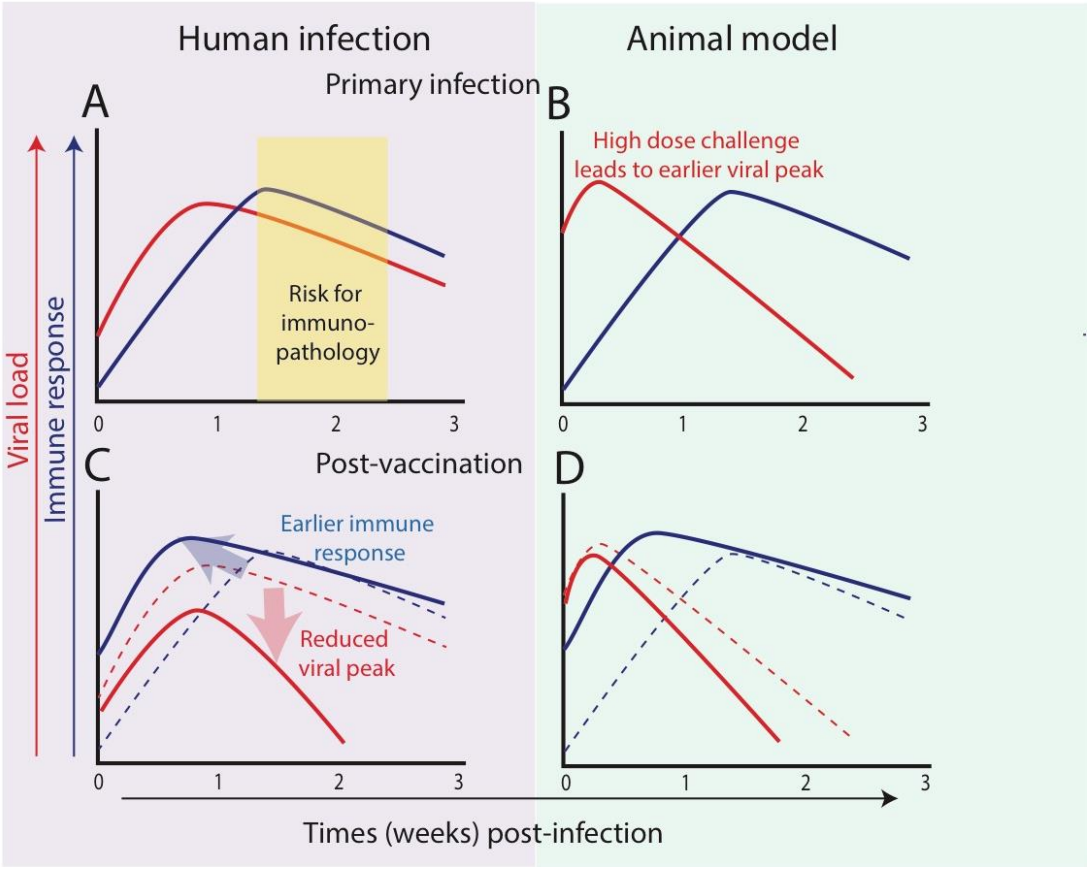

Supplementary Methods

For Figure 2d, data were extracted from the original publications using an online digitizer tool (https://apps.automeris.io/wpd/). All Ct values were converted into RNA equivalent copies per ml quantity according to[1]. A linear regression was used to obtain a parametric relationship between log10 RNA copies per ml and Ct values:
Log 10 VL = 14.11 – 0.3231 Ct

Extracted data showed considerable variability and contained values below detection limits. Before fitting, we performed a log transformation of the non-zero data and employed a censored regression method to accommodate values below the lower limit of detection. More specifically, a censored regression method was used to estimate the decay slope from peak in the extracted viral load data. In some studies[2-4], where longitudinal data was obtainable (because there were no overlapping data points, with clear distinction between patients, or because the raw data was available), a censored mixed effect model (with random intercepts and slopes) was used to estimate the decay rate. This was performed using the *CensReg* (normal censored regression) and *lmec* (mixed effect censored regression) libraries in *R* (v3.63).

References

1 Zost, S. J. *et al.* Potently neutralizing and protective human antibodies against SARS-CoV-2. *Nature*, doi:10.1038/s41586-020-2548-6 (2020).

2 Woolsey, C. *et al.* Establishment of an African green monkey model for COVID-19. Preprint at bioRxiv, doi:10.1101/2020.05.17.100289 %J (2020).

3 Wolfel, R. *et al.* Virological assessment of hospitalized patients with COVID-2019. *Nature* **581**, 465-469 (2020).

4 To, K. K. *et al.* Consistent detection of 2019 novel coronavirus in saliva. *Clin Infect Dis*, doi:10.1093/cid/ciaa149 (2020).

Data was extracted from:

Animal models	Reference
Mouse (transgenic hACE2)	Bao, L. *et al.* The Pathogenicity of SARS-CoV-1 2 in hACE2 Transgenic Mice. Preprint at *BioRxiv*, doi:10.1101/2020.02.07.939389 (2020).
Golden hamster	Sia, S. F. *et al.* Pathogenesis and transmission of SARS-CoV-2 in golden hamsters. *Nature*, doi:10.1038/s41586-020-2342-5 (2020).
Syrian hamster	Chan, J. F. *et al.* Simulation of the clinical and pathological manifestations of Coronavirus Disease 2019 (COVID-19) in golden Syrian hamster model: implications for disease pathogenesis and transmissibility. *Clin Infect Dis*, doi:10.1093/cid/ciaa325 (2020).
Ferret	Kim, Y.-I. *et al.* Infection and Rapid Transmission of SARS-CoV-2 in Ferrets. *Cell Host & Microbe*, doi:10.1016/j.chom.2020.03.023 (2020).
Macaque	Bao, L. *et al.* Lack of Reinfection in Rhesus Macaques Infected with SARS-CoV-2. Preprint at *bioRxiv*, doi:10.1101/2020.03.13.990226 (2020).
Cynomolgus macaque	Rockx, B. *et al.* Comparative pathogenesis of COVID-19, MERS, and SARS in a nonhuman primate model. *Science* **368**, 1012-1015, doi:10.1126/science.abb7314 (2020).
Rhesus macaque	Munster, V. J. *et al.* Respiratory disease in rhesus macaques inoculated with SARS-CoV-2. *Nature*, doi:10.1038/s41586-020-2324-7 (2020).

Patient number / source of sample	
96 pts, stool	Zheng, S. *et al.* Viral load dynamics and disease severity in patients infected with SARS-CoV-2 in Zhejiang province, China, January-March 2020: retrospective cohort study. *BMJ* **369**, m1443, doi:10.1136/bmj.m1443 (2020).
N = 9, sputum, stool, and throat swab	Wolfel, R. *et al.* Virological assessment of hospitalized patients with COVID-2019. *Nature* **581**, 465-469, doi:10.1038/s41586-020-2196-x (2020).
N=12, saliva	To, K. K. *et al.* Consistent detection of 2019 novel coronavirus in saliva. *Clin Infect Dis*, doi:10.1093/cid/ciaa149 (2020).
N=18, nose and throat swabs	Zou, L. *et al.* SARS-CoV-2 Viral Load in Upper Respiratory Specimens of Infected Patients. *New England Journal of Medicine* **382**, 1177-1179, doi:10.1056/NEJMc2001737 (2020).
N=31, nasopharyngeal swab	Zhou, R. *et al.* Viral dynamics in asymptomatic patients with COVID-19. *Int J Infect Dis* **96**, 288-290, doi:10.1016/j.ijid.2020.05.030 (2020).
N=30, saliva and endotracheal aspirate	To, K. K.-W. *et al.* Temporal profiles of viral load in posterior oropharyngeal saliva samples and serum antibody responses during

	infection by SARS-CoV-2: an observational cohort study. *The Lancet Infectious Diseases* **20**, 565-574, doi:10.1016/s1473-3099(20)30196-1 (2020).
N=51, throat swab	Xu, T. *et al.* Clinical features and dynamics of viral load in imported and non-imported patients with COVID-19. *Int J Infect Dis* **94**, 68-71, doi:10.1016/j.ijid.2020.03.022 (2020).
N=44, saliva and nasopharyngeal swab	Wyllie, A. L. *et al.* Saliva is more sensitive for SARS-CoV-2 detection in COVID-19 patients than nasopharyngeal swabs. Preprint at medRxiv doi:10.1101/2020.04.16.20067835 (2020).
N=21, nasopharyngeal swab	Chamieh, A. *et al.* Viral Dynamics Matter in COVID-19 Pneumonia: the success of early treatment with hydroxychloroquine and azithromycin in Lebanon. Preprint at *medRxiv*, doi:10.1101/2020.05.28.20114835 (2020).